EX/1-3

Steady State High β_N Discharges and Real-Time Control of Current Profile in JT-60U

T. Suzuki 1), A. Isayama 1), Y. Sakamoto 1), S. Ide 1), T. Fujita 1), H. Takenaga 1), T. C. Luce 2), M. R. Wade 3), T. Oikawa 1), O. Naito 1), S. Sakata 1), M. Sueoka 1), H. Hosoyama 1), M. Seki 1), N. Umeda 1), T. Ozeki 1), K. Kurihara 1), T. Fujii 1), T. Yamamoto 1), and the JT-60 Team 1)

1) Japan Atomic Energy Research Institute, Naka, Ibaraki 311-0193, Japan
2) General Atomics, San Diego, California 92186, USA
3) Oak Ridge National Laboratory, Oak Ridge, Tennessee 37831, USA

e-mail contact of main author: suzukit@fusion.naka.jaeri.go.jp

Abstract. The sustainment of the high normalized beta value β_N has progressed remarkably in JT-60U. β_N=3 was sustained for 6.2s and β_N=2.5 for 15.5s, and β_N=2.1 for 20 s, only interrupted by the capability of neutral beam heating system (power and pulse length), not by the plasma stability, with low safety factor (q_{95}=2.2, 3.4, and 3.2, respectively). In the case of β_N=2.1, in particular, the current profile reached a steady state. In this low safety factor regime, the resonant surfaces with q=3/2 and 2/1 were shifted outside the steep pressure gradient layer, stabilizing the neoclassical tearing mode (NTM) above the previous β_N-limit imposed by NTMs. To establish the feedback control of the safety factor profile q(ρ), a real-time q(ρ) control system has been developed using the motional Stark effect (MSE) diagnostic as detector and the lower hybrid current drive (LHCD) as actuator. For the first time, real-time feedback control has been demonstrated based on local pitch angle measurement and control of parallel refractive index of LH waves adjusting the LHCD location.

1. Introduction

Magneto-hydro-dynamical (MHD) stability of plasma directly affects economy of fusion reactors. Since current density and pressure profiles in a tokamak plasma determine the MHD stability, appropriate profiles are necessary to achieve higher stability. While the pressure profile relaxes in a time scale of energy confinement time τ_E, current profile relaxes in current diffusion time τ_R, much longer than τ_E. Therefore, the stability of plasma to be extrapolated to that of steady fusion reactors must be discussed in the time scale of τ_R that takes longer period to reach a steady state. This paper handles roles of current profile, especially the steady state current profile, on sustaining high stability, or the normalized beta β_N.

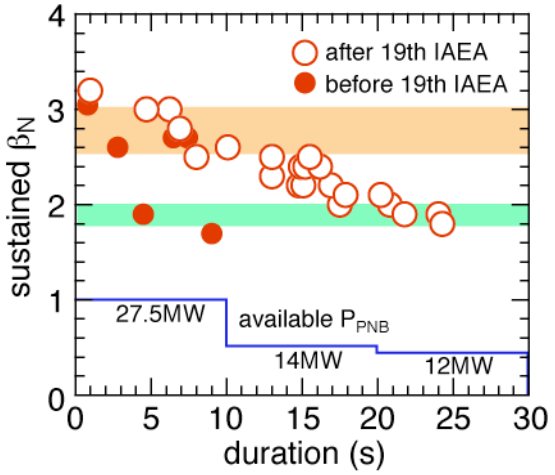

FIG. 1. Extended operation regime toward higher β_N and its longer sustainment. The sustained period longer than 10s has been realized by the long-pulse modification. Available P-NB power as a function of heating period is indicated in the figure.

In 2003, modifications in operational control systems were made for longer discharges for this study. The JT-60U machine capability was improved; the discharge duration was extended up to 65 s (formerly 15 s) and the NB/RF heating duration up to 30s/60s (formerly 10 s both). Utilizing this capability, we have expanded the operation regime towards higher β_N and longer sustainment

than those in the last IAEA conference. Figure 1 shows progress of sustained period. Most of the discharges after the modification exhibit quasi-steady/steady feature for current diffusion. In addition, in β_N=3 case, lower q_{95} operation than conventional tokamak scenario made it possible to avoid alignment of rational surface and steep pressure gradient location, and to obtain broad pressure profile. This implies that optimization of current / pressure profile raises the β_N limit even in quasi-steady state for current evolution. While the discharges shown in Fig. 1 employ pre-programmed heating or current drive (CD) to achieve a relaxed current profile, active feed back control of current profile will be important to obtain an optimized current profile for much higher β_N. For this purpose, real-time feed back control system of current profile has been developed. Controllability of q profile is examined. The final goal for the current profile control system is to sustain a current profile optimized for high stability.

Section 2 describes steady sustainment of the high β_N plasma. Steady state of current profile was found to essential for the sustainment. In section 3, a quasi-steadily sustained discharge with high β_N of 3 is examined. Real-time control of current profile is described in section 4. We conclude with a summary in section 5.

2. Steady sustainment of high β_N and effect of current profile evolution on sustainable β_N

As shown in Fig. 1, β_N=2.5 has been sustained for 15.5s, a factor of two longer than that was reported in the last conference [2]. Figure 2 shows waveforms of the high β_p H-mode plasma (E043903) having I_p=0.9MA and B_t=1.7T (q_{95}=3.4). The sustained period is restricted by the available heating power, comprising positive ion based neutral beam heating (P-NB) [9], negative ion based NB heating (N-NB) [8], and electron cyclotron (EC) heating [10]. In case of such long NB heating, rise in NB-facing-wall temperature due to shine-through loss of the NB can restrict its injection duration, and hence the available heating power, so that plasma density and path-length of NB had to be optimized. There was no significant electro-magnetic instability observed by pick-up coils. Although EC waves are continuously injected, the sustainment of β_N is not a result of suppression/stabilization of a neo-classical tearing mode

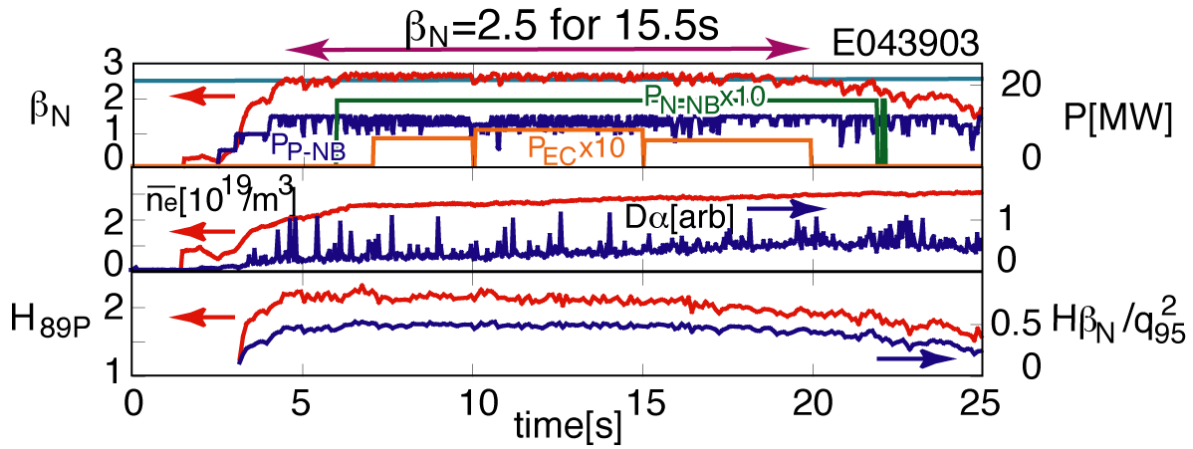

FIG. 2. Temporal evolutions of β_N, injection power (P-NB, N-NB, EC), line averaged electron density, D_α intensity, H-factor, and $H\beta_N/q_{95}^2$. Sustained duration of β_N=2.5 reached 15.5s, during which H_{89P} and $H_{89P}\beta_N/q_{95}^2$ were 1.9-2.3 and 0.4-0.5, respectively. Electron density continuously increased from 55% to 80% of Greenwald density due to the increased recycling.

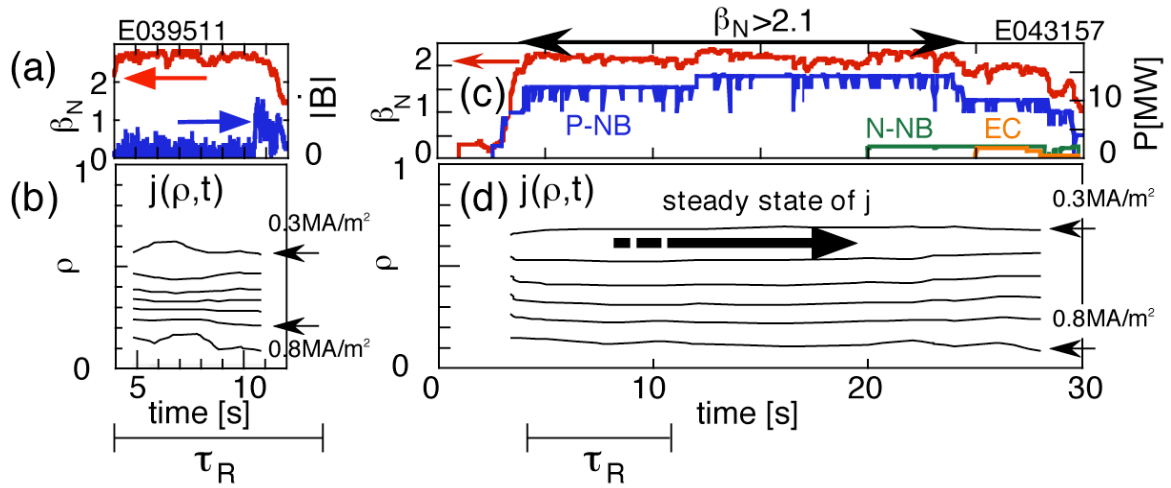

FIG. 3. (a) Temporal evolution of normalized beta (β_N) and amplitude of magnetic fluctuation of n=2 mode. (b) Temporal evolution of current profile j(ρ,t) evaluated using MSE in the same discharge in (a). (c) Temporal evolution of β_N., where β_N=2.1 was sustained for 20s. (d) Temporal evolution of j(ρ,t) in the same discharge in (c). The current profile has achieved a steady state after 10s after β_N reached 2.1.

(NTM), since resonance location of the EC waves was not at the rational surfaces, such as q=1.5 or 2. This discharge exhibits not only high β_N, but also high confinement H_{89P}=1.9-2.3 and high $H_{89P}\beta_N/q_{95}^2$=0.4-0.5 during the sustainment, where the latter is a measure of fusion gain. As shown in Fig. 2, the intensity of the D_α emission continuously increased, in spite that there was no gas puffing and only NB fueling. Due to the increased recycling, line averaged electron density continuously increased from $1.9\text{x}10^{19}\text{m}^{-3}$ to $2.9\ \text{x}10^{19}\text{m}^{-3}$, corresponding to Greenwald density fraction of 55% and 80%, respectively. During t=7-20s (nearly constant heating power), the electron density increased by 15% and H_{89P} degraded by 15%. Electron density profile increased from the edge to the center, and electron and ion temperature profiles decreased from the edge to the center.

Resistive diffusion time, defined by $\tau_R=\mu_0\sigma_{NC}(r=a/2)(a/2)^2$, was 8.9s, so that the sustained period corresponds to $1.7\tau_R$. In the above equation, a is averaged minor radius and $\sigma_{NC}(r=a/2)$ is the neoclassical conductivity at half minor radius. Although no NTM occurred in E043903 shown in Fig. 2, NTM suddenly appeared after β_N=2.7 was sustained for 6.5s (E039511; q_{95}=3.6, I_p=1MA, B_t=2T), as shown in Fig. 3(a). This could be due to a gradual evolution of current profile j(ρ,t), as shown in Fig. 3(b), even with β_N kept constant. The sustained period of 6.5s corresponds to $0.68\tau_R$, and was shorter than current diffusion time. It was found that temporal evolution of the current profile plays an important role in stable sustainment of the plasma.

We could obtain a longer sustained period of 20s at β_N=2.1 (E043157, Ip=1.0MA, Bt=1.7T). Figure 3(c) shows waveforms of the discharge. The current and pressure profiles at β_N=2.1 have reached a steady state. Current density profile j(ρ) has reached a steady state after 10s after β_N reached 2.1 in Fig. 3(d). The steady state was not interrupted by the appearance of instability, but by the limit of heating system (12-14MW). The resistive diffusion time τ_R as described above is indicated by bars in Fig. 3. Sustained period of 20s for β_N=2.1 corresponds to $3.1\tau_R$. Although P-NB heating power decreased at t=24s, a combination of N-NB and EC

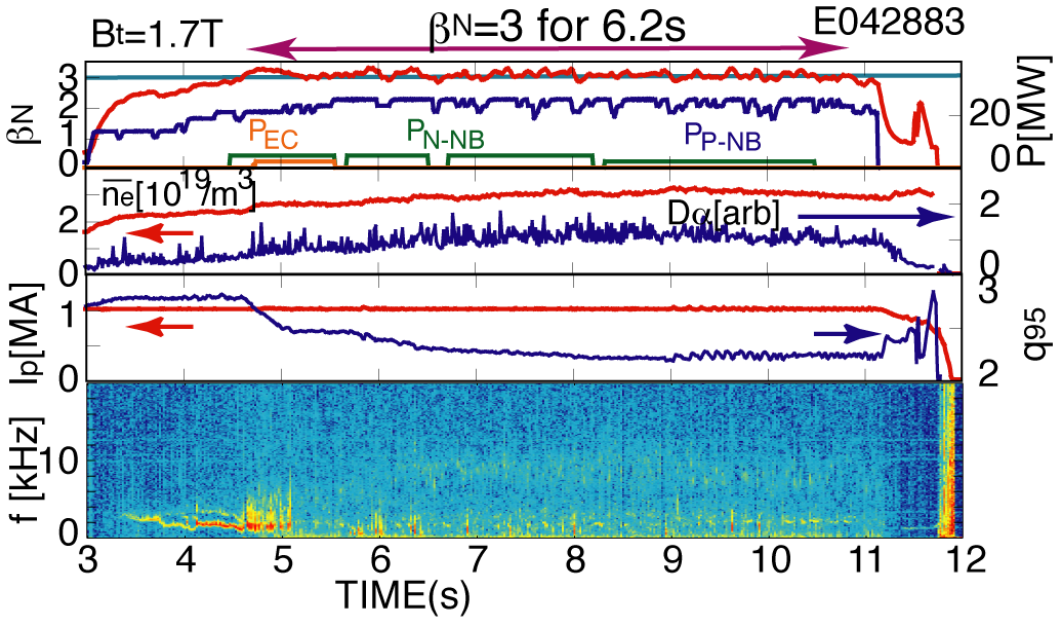

FIG. 4. Temporal evolution of β_N, injection power, line-averaged electron density, D_α intensity, plasma current and safety factor at 95% of magnetic flux. Bottom figure shows temporal evolution of the spectrum of magnetic fluctuation (dB/dt). Red (blue) indicates strong (weak) intensity.

heating has extended the duration further up to 24s with β_N=1.9, which is similar to a goal beta for ITER inductive operation with Q=10.

3. Stable higher β_N (β_N=3) operation at low safety factor regime

As plotted in Fig. 1, we could also extend a sustained duration at a higher β_N. β_N=3 has been sustained for 6.2s in a quasi-steady-state (E042883), again, only interrupted by the limit of heating at 23-25MW to sustain β_N=3. In the last conference, we reported that the period of β_N=3 was interrupted by NTM at 0.8s [1]; β_N up to 2.7 was sustained in a quasi-steady-state (7.4s) [2]. Figure 4 shows waveforms of the discharge, with magnetic fluctuation spectrum at the bottom. Although 3/2 NTM appeared in the initial phase of the sustainment (t<5s), the NTM disappeared along with decrease of q_{95}. Low q operation (q_{95}=2.2, I_p=1MA, B_t=1.7T) has shifted the NTM resonant rational surfaces (q=3/2, 2/1) outward, because the q_{95} got smaller keeping q(0)~1. Figure 5 shows safety factor and pressure gradient profiles. The low q_{95} operation helped to avoid alignment of the steep pressure gradient region and the rational surfaces. Under an inappropriate q profile, in the case of β_N=3, NTM appeared immediately in 0.8s. Moreover, the pressure profile was broadened in E042883, and

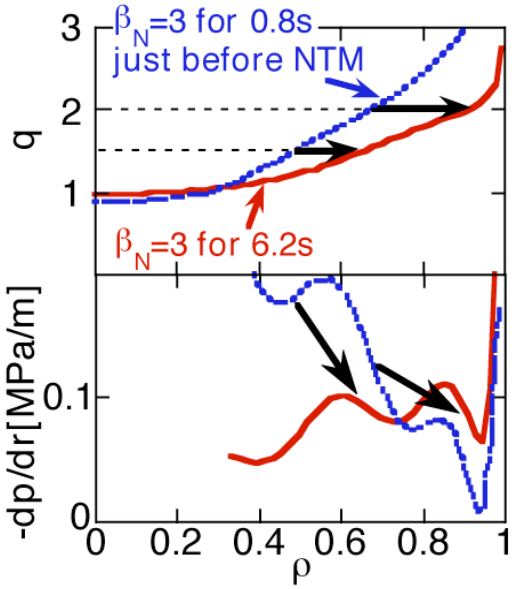

FIG. 5. Safety factor and pressure gradient profiles with β_N=3 sustained for 6.2s (solid; E042883), in comparison with the case with β_N=3 sustained for 0.8s just before NTM onset (dotted; E039505).

the pressure gradient was lowered (Fig. 5), since paths of heating NBs changed from the on-axis to the off-axis; decreasing minor radius due to down shift of magnetic axis caused decrease in q_{95}.

Concern in such a low q operation has been sawtooth instability with large inversion radius that could lead to loss of high temperature core plasma. There was no significant sawtooth activity observed in E042883. Since it seemed quite curious, from the viewpoint of conventional tokamak operation, that no sawtooth activity was detected in such a low q_{95}~2.2 plasma, we examined a steady current profile. Beam driven current and bootstrap current profiles were calculated using orbit following Monte Carlo (OFMC) code and ACCOME code [7], respectively. The steady state Ohmic current profile was calculated under spatially uniform toroidal electric field, assuming the neo-classical conductivity profile. Sum of the calculated beam driven, bootstrap, and Ohmic current profile agreed with experimental current profile evaluated using the motional Stark effect (MSE) diagnostic [11,12]; q(0) was about unity as shown in Fig. 5. Because electron temperature at the center was low due to the off-axis NB heating, conductivity at the center was low. Thus, current profile in the plasma is in a quasi-steady state with q(0)~1 and q_{95}=2.2, and we expect current does not concentrate any more into the axis, and hence, sawtooth activity was not observed. This discharge implies a possibility to achieve and sustain high β_N without help of NTM suppression by EC current drive

4. Real-time control of safety factor profile for stable sustainment of current profile

As described in Sec. 3, an optimization of the current profile could raise β_N limited by instabilities, such as NTM and sawtooth. A way to optimize and to sustain the current profile is actively control of the current/safety factor profile. The goal of this study is to robustly sustain the optimized current profile, even if there exist perturbation of current profile. A real-time q(ρ) control system has been developed; this system enables real time evaluation of q(ρ) by MSE diagnostic and control of CD location by adjusting the parallel refractive index $N_{//}$ of lower-hybrid (LH) waves through the change of phase difference (Δϕ) of LH waves between multi-junction launcher modules [3]. The control system controls ρ_{CD} through $N_{//}$ (or directly Δϕ) in such a way to minimize the difference between the real-time evaluated q(ρ) and the reference $q_{ref}(\rho)$.

For the first time, q(ρ) has been evaluated in real time from the local measurement of pitch angle by MSE. The equilibrium was not reconstructed in real-time with MSE, but q(ρ) was estimated under an assumption that the shape of the last closed flux surface (LCFS) represents the shapes of internal magnetic surfaces. The following shape of magnetic surface was assumed, taking account of elongation κ, triangularity δ, and Shafranov shift profile $\Lambda(\rho) \equiv (R_p - R_{ax})\rho^2$;

$$R = R_{ax} + \Lambda(\rho) + a\rho\cos(\theta + \delta sin\theta),$$

$$Z = Z_{ax} + a\rho\kappa sin\theta.$$

Cauchy condition surface (CCS) method [6] was employed to calculate the shaping parameters of the LCFS, such as major radius of geometric center R_p, major radius (vertical position) of the magnetic axis R_{ax} (Z_{ax}), a, κ, and δ. The magnetic axis by the CCS method is a weighted center of the plasma current. Safety factor at each MSE channel location (R, Z) is calculated on the nested magnetic surfaces, using local pitch angle measured by MSE diagnostic. The calculation

is finished within every 10ms. Figure 6 shows safety factor by real-time evaluation, in comparison with that by equilibrium reconstruction. They show a good agreement in a wide range of plasma parameters (I_p=0.6-1.0MA, B_t=1.7-2.4T, β_p=0.3-0.8). Since the safety factor is inversely proportional to the poloidal magnetic field, which is a spatial integral of current density, we can also evaluate current density profile in real-time. When change in current by penetration of Ohmic current is weaker than that by non-inductive current, minor radius of the CD location ρ_{CD} is represented by a minor radius where temporal increment of current density becomes maximum. This method to detect the CD location is similar to that we had already reported in the references [4,5], except that the detection of ρ_{CD} here was performed in real-time.

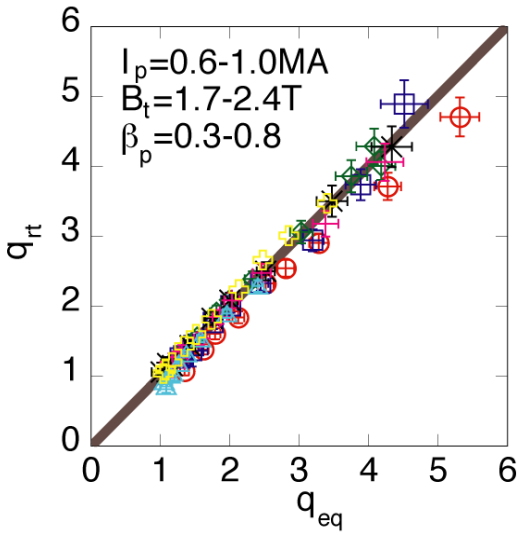

FIG. 6. Comparison of the safety factor by the real-time calculations (q_{rt}) and by the equilibrium reconstructions (q_{eq}) under wide variety of plasma parameters (I_p, B_t, and β_p).

Using the above technique, we constructed a q(ρ) control system. The system compares the real-time q(ρ) and given reference $q_{ref}(\rho)$ with a given weight w(ρ), and detects a location where a residual $(q(\rho)-q_{ref}(\rho))w(\rho)$ is maximum; the weight is given considering an accuracy of the q(ρ) at the location and importance on the control. For example, the weight at the plasma edge is small, since edge safety factor is not controllable, but dominated by total plasma current. In order to reduce the largest residual, control system determines a reference location ρ_{CDref} where current is driven. The CD location ρ_{CD} detected in real-time should agree to the reference location ρ_{CDref}, so that a feed back control is applied to Δφ, which affects ρ_{CD}; changing rate $d\Delta\phi/dt$ is proportional to $\rho_{CD}-\rho_{CDref}$. We must note that the above control logic is not restricted to LHCD as an actuator. If a current driver has any controllable parameter to change its driven current location, the current driver can be easily built into the system. Finally, in case of LHCD, injection power P_{LH} is another controllable parameter. In order to keep plasma loop voltage constant, P_{LH} was controlled so as not to change LH driven current I_{LH}, even if Δφ or $N_{//}$ changed; LHCD efficiency $I_{LH}n_eR_p/P_{LH}$ is proportional to $<1/N_{//}^2>$ [13], where $<1/N_{//}^2>$ is an average of $1/N_{//}^2$ weighted by LH power spectrum.

The above described control of q profile has been applied to a plasma (E044011) having Ip=0.6MA, Bt=2.3T. Electron density was controlled to $n_e=0.5\times10^{19}m^{-3}$ by gas-puffing. Gap width between the launcher and the plasma surface was also controlled in order to obtain a good coupling of LH waves to the plasma. Frequency of the LH waves is 2.0GHz in JT-60U. Figure 7 shows temporal evolution of q(ρ). The number of MSE channels used for the control was 9 for the discharge, covering ρ~0.1-0.7 in minor radius. Reference q profile was set to a monotonic positive magnetic shear having q(0)=1.5. Co-LHCD (maximum injection power P_{LH}=1MW) has been applied during 4s<t<27s, and real-time control of q(ρ) has started at t=4.5s. We intended to vanish q=1.5 surface which can be resonant to m/n=3/2 instability, such as NTM. At the initial phase of q(r) control (t<15s), LH power was not injected into the plasma due to

break down in the LH antenna. After t=15s, plasma loop voltage dropped with increase in injection power. Safety factor at the center was raised from 1.1 to 1.3. The control system itself determined $N_{//}$ (or directly controllable $\Delta\phi$). The largest residual, $\max((q(\rho)-q_{ref}(\rho))w(\rho))$, decreased down to a level which is about two times larger than error of $q(\rho)$ measurement, in a time scale longer than 5s. The safety factor profile did not reach the reference $q_{ref}(\rho)$, since the available LH power was limited in this discharge.

5. Summary

The JT-60U machine capability was improved toward long pulse operation reaching steady state of current diffusion; the discharge duration was extended up to 65 s (formerly 15s) and the NB heating duration up to 30s (formerly 10 s). Utilizing this capability, we have expanded the operation regime towards high β_N and long sustainment. β_N=2.5 (H_{89P}=1.9-2.3, $H_{89P}\beta_N/q_{95}^2$=0.4-0.5, Greenwald fraction of 0.55-0.8) was sustained for 15.5s, β_N=1.9 for 24s. Current profile reached steady state for the latter case. Low q_{95} operation enabled us to sustain β_N=3 for 6.2s, avoiding NTM. Sawtooth activity was not observed. This discharge implies a possibility to achieve and sustain high β_N without help of NTM suppression by EC current drive. Real-time control system of safety factor profile has been developed. The system consists of 1) calculation of the safety factor profile and current drive location using MSE diagnostic, and 2) control of CD location by the control of the parallel refractive index of LH

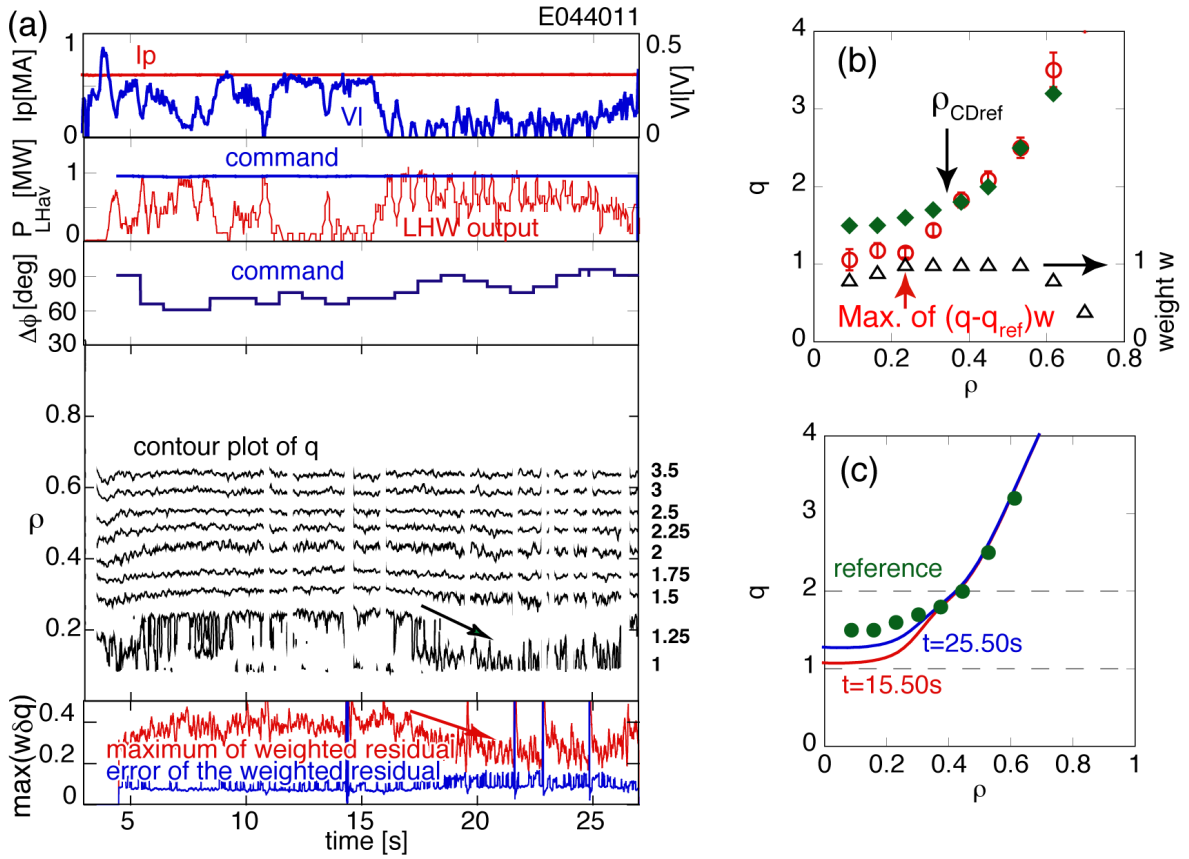

FIG. 7. (a) Waveforms of plasma current, loop voltage, LH power, phase difference between launcher modules, contour plot of safety factor profile, and maximum of residuals between q by real-time calculation and reference q. (b) Safety factor profile by real-time calculation (circles), and the reference q profile (rectangles). Triangle symbols show the weight w. (c) safety factor profile at t=15.5s and 25.5s.

waves. Safety factor at the center q(0) was raised from 1.1 to 1.3. Real-time q(ρ) control experiment continues for the demonstration of control at high β plasma.

References

[1] FUJITA, T., and the JT-60 Team, Nucl. Fusion **43** (2003) 1527.
[2] ISAYAMA, A., et al., Nucl. Fusion **43** (2003) 1272.
[3] SEKI, M., et al., Fusion Sci. Tech. **42** (2002) 452.
[4] SUZUKI, T., et al., Nucl. Fusion **44** (2004) 699.
[5] SUZUKI, T., et al., J. Plasma Fusion Res. **80** (2004) 362.
[6] KURIHARA, K., et al., Fusion Tech. **34** (1998) 548.
[7] TANI, K., et al., J. Computational Phys. **98** (1992) 332.
[8] KURIYAMA, M., et al., Fusion Sci. Tech. **42** (2002) 410.
[9] KURIYAMA, M., et al., Fusion Sci. Tech. **42** (2002) 424.
[10] IKEDA, Y., et al., Fusion Sci. Tech. **42** (2002) 435.
[11] SUGIE, T., et al., Fusion Sci. Tech. **42** (2002) 482.
[12] FUJITA, T., et al., Fusion Eng. Des. **34-35** (1997) 289.
[13] USHIGUSA, K., et al., Fusion Sci. Tech. **42** (2002) 255.